Visual Cone Arrestin 4 Contributes to Visual Function and Cone Health

Janise D. Deming,[1] Joseph S. Pak,[1] Bruce M. Brown,[1] Moon K. Kim,[2] Moe H. Aung,[3] Yun Sung Eom,[1,4] Jung-a Shin,[1,5] Eun-Jin Lee,[1,6] Machelle T. Pardue,[2,3] and Cheryl Mae Craft[1,7]

[1]Mary D. Allen Laboratory for Vision Research, USC Eye Institute, Department of Ophthalmology, Keck School of Medicine of the University of Southern California, Los Angeles, California, United States
[2]Rehabilitation Research & Development Center of Excellence, Atlanta VA Medical Center, Decatur, Georgia, United States
[3]Neuroscience/Ophthalmology, Emory University, Atlanta, Georgia, United States
[4]Dornsife College of Letters, Arts and Sciences, University of Southern California, Los Angeles, United States
[5]Department of Anatomy, School of Medicine, Ewha Womans University, Seoul, Korea
[6]Department of Biomedical Engineering, University of Southern California Viterbi School of Engineering, Los Angeles, California, United States
[7]Department of Cell & Neurobiology, Keck School of Medicine of the University of Southern California, Los Angeles, California, United States

Correspondence: Cheryl Mae Craft, USC Eye Institute, Department of Ophthalmology, Keck School of Medicine of the University of Southern California, IGM, 2250 Alcazar Street, Mail Code: 9075, Clinical Sciences Center 135H, Los Angeles, CA 90033, USA; CherylMae.Craft@med.usc.edu, eyesightresearch@hotmail.com.

JDD and JSP contributed equally to the work presented here and should therefore be regarded as equivalent authors.

Submitted: February 9, 2015
Accepted: June 30, 2015

Citation: Deming JD, Pak JS, Brown BM, et al. Visual cone arrestin 4 contributes to visual function and cone health. *Invest Ophthalmol Vis Sci*. 2015;56:5407–5416. DOI:10.1167/iovs.15-16647

Purpose. Visual arrestins (ARR) play a critical role in shutoff of rod and cone phototransduction. When electrophysiological responses are measured for a single mouse cone photoreceptor, ARR1 expression can substitute for ARR4 in cone pigment desensitization; however, each arrestin may also contribute its own, unique role to modulate other cellular functions.

Methods. A combination of ERG, optokinetic tracking, immunohistochemistry, and immunoblot analysis was used to investigate the retinal phenotypes of *Arr4* null mice (*Arr4*$^{-/-}$) compared with age-matched control, wild-type mice.

Results. When 2-month-old *Arr4*$^{-/-}$ mice were compared with wild-type mice, they had diminished visual acuity and contrast sensitivity, yet enhanced ERG flicker response and higher photopic ERG b-wave amplitudes. In contrast, in older *Arr4*$^{-/-}$ mice, all ERG amplitudes were significantly reduced in magnitude compared with age-matched controls. Furthermore, in older *Arr4*$^{-/-}$ mice, the total cone numbers decreased and cone opsin protein immunoreactive expression levels were significantly reduced, while overall photoreceptor outer nuclear layer thickness was unchanged.

Conclusions. Our study demonstrates that *Arr4*$^{-/-}$ mice display distinct phenotypic differences when compared to controls, suggesting that ARR4 modulates essential functions in high acuity vision and downstream cellular signaling pathways that are not fulfilled or substituted by the coexpression of ARR1, despite its high expression levels in all mouse cones. Without normal ARR4 expression levels, cones slowly degenerate with increasing age, making this a new model to study age-related cone dystrophy.

Keywords: cone arrestin, visual function, cones, age-related cone degeneration

Arrestins compose a family of four proteins that are essential for desensitization of numerous G-protein coupled receptors (GPCRs). In mammals, there are two visual arrestins, Arrestin 1 (ARR1, also called S-Antigen or 48 kilo Dalton protein)[1–3] and Arrestin 4 (ARR4, also called cone arrestin [CAR], X-arrestin, or *ARR3* in the NCBI gene nomenclature).[4,5] Previous work clearly demonstrated the functional roles of visual arrestins in mouse models in which these two genes are individually or simultaneously ablated (*Arr1*$^{-/-}$, *Arr4*$^{-/-}$, or *Arr1*$^{-/-}$*Arr4*$^{-/-}$).[6–9]

After opsins have been light-activated, their shutoff begins with multiple phosphorylations by G-protein coupled receptor kinase 1 (Grk1) for rhodopsin,[10,11] and depending on the species, either Grk1 or Grk7 for cone opsins.[12–16] These phosphorylated opsins are subsequently bound by either ARR1 or ARR4, which are sterically inhibited from further activation of the downstream G-protein, alpha (α) transducin. Arrestin 1 is primarily responsible for the signal shutoff of rhodopsin in rods; in contrast, in murine cones both ARR1 and ARR4 are coexpressed and desensitize short (S-) or middle (M-) wavelength opsins.[8] Compared with ARR4, ARR1 has a 50-fold higher concentration in cone photoreceptors and can substitute for ARR4 in the shutoff of S- or M-opsin.[8] When measuring the single cone photoreceptor physiological response after a bright light stimulus, experiments demonstrate that mice without expression of both visual arrestins have limited and delayed recovery, underscoring the critical role of the visual arrestins in normal phototransduction shutoff.

Recent evidence suggests that ARR4 plays a unique role in other visual functions for which ARR1 cannot substitute and vice versa. Zebrafish retina studies of the ARR4 ortholog, Arr3a, have demonstrated that it plays a vital role in maintaining the

normal optokinetic response of zebrafish larvae across temporal frequencies.[17] In contrast, ARR1, but not ARR4, was shown to modulate the mouse rod photoreceptor presynaptic exocytotic synaptic function of N-ethylmaleimide sensitive factor (NSF) and to contribute to normal light adaptation.[7,9]

In this study, we further investigated *Arr4*$^{-/-}$ mice[8] to assess the contribution of ARR4 to overall cone visual function. In previous published work, *Arr4*$^{-/-}$ mice had enhanced photopic ERG amplitudes and abnormal flicker response compared to controls (WT).[7] We performed optokinetic tracking (OKT) studies to determine if these abnormal photopic ERG amplitudes corresponded to downstream functional changes in either visual acuity or contrast sensitivity. We also examined the cone photoreceptor morphology of *Arr4*$^{-/-}$ mice as they age, to determine if the observed abnormal retinal physiology and behavioral defects in younger mice contributed to greater visual deficits or increased cone degeneration over time.

Materials and Methods

Mice

Mice that were *Arr4*$^{-/-}$ were produced on a mixed C57Bl/6J-129SVJ strain (WT) background[8] and reared in a 12 hour: 12-hour light/dark cycle and tested at age 2, 4, 7, and 9 months. The mice tested for OKT were 3 to 4 months old. The 2- and 4-month-old mice were phenotypically identical, as were the 7- and 9-month-old mice, so they were separated into two groups: "younger" mice aged 2 and 4 months and "older" mice aged $\geq$7 months. Mice of either sex were used for experimental procedures. All animals were treated according to the guidelines established by the Institute for Laboratory Animal Research (Guide for the Care and Use of Laboratory Animals), conformed to the ARVO Statement for the Use of Animals in Ophthalmic and Vision Research, and were approved by the appropriate animal committees of the University of Southern California and the Atlanta VA Medical Center.

Optokinetic Tracking (OKT)

For optokinetic tracking, mice were placed on a platform in the center of a virtual-reality chamber, which is composed of four computer monitors (OptoMotry; Cerebral Mechanics, Lethbridge, AB, Canada), as previously described.[18] A vertical sine wave grating rotated across the monitors at a speed of 12°/s. Mice were monitored for reflexive head movements in the direction of the rotating gratings using a video camera positioned above the animal. For visual acuity assessment, the grating started at a 0.042 cyc/deg spatial frequency with 100% contrast and increased in a staircase paradigm until the maximum spatial frequency threshold was reached. Contrast sensitivity curves were measured across five spatial frequencies (0.031, 0.064, 0.092, 0.103, and 0.192 cyc/deg).[19]

ERG Analysis

Following 12 hours of dark adaptation, ERG studies were performed as previously described in detail.[7] Briefly, white background light at 8 foot candle (200 cd) was delivered through one arm of a bifurcated glass fiber optic for 1 minute before the first flash response was recorded, and this background light remained on throughout all recordings. Flash stimuli of 10 μs duration, from 0.2 to 20 Hz, were delivered through the other arm of the fiber optic. The source of the flash stimuli was a Xenon flash bulb with the ultraviolet filter removed in order to permit transmittance of shorter wavelengths (<400 nm). The delivery arm of the fiber optic was affixed to the flash unit directly under and 7 cm from the Xenon flash bulb. Additional flash responses were recorded every 2 minutes after the first flash until 15 minutes of light adaptation (Supplementary Figs. S3A, S3B). The light-adapted single-flash recordings were taken 1 minute after the light adaptation recordings concluded (16 minutes total of light adaptation). Maximum flash intensity at the surface of the cornea was 2.01 log (scot cd/m^2) and calibrated with a photometer (model S350 laboratory photometer with a model 211 illuminance sensor head; UDT Instruments, San Diego, CA, USA). For some studies, reduction in intensity (from 2.01 to −1.59 log scot cd/m^2) was achieved by the use of both neutral density Wratten filters and the 16X to 1X flash intensity settings on the Grass visual stimulator. The optimal flash intensity that resulted in the greatest difference between young WT and young *Arr4*$^{-/-}$ b-wave amplitude was 2.01 log (scot cd/m^2; Supplementary Fig. 2D), so this was the intensity used for the studies presented here.

The brighter background light was intended to saturate the rods and minimize the contribution of rod signal to the photopic ERG. The amount of background light used for this purpose varies from study to study, and 200 cd/m^2 is at the higher end of this range. However, we have no evidence that this higher background light has a deleterious effect on cone function. An analysis of background light levels showed that the shape of the ERG does not change with background light at this level, although implicit times may be decreased.[20]

Immunoblot Analysis

Each eye was enucleated and the retina removed. After dissection, each retina was flash frozen on dry ice and maintained at −80°C until use. Each frozen retina was homogenized; 60 μg of protein per retina were resolved on replicate 10% SDS-PAGE, transferred to nitrocellulose membranes (LI-COR Biotechnology, Lincoln, NE, USA), incubated sequentially with antibodies for anti β-actin (1:4000) and either anti-S-opsin (1:5000), or anti-M-opsin (1:5000).[16] Appropriate secondary antibodies conjugated to a fluorophore (680 nm or 800 nm) allowed detection using an infrared detection system (Li-Cor Odyssey; LI-COR Biotechnology). We used imaging software (Image Studio, LI-COR Biotechnology) to quantify the intensity of each band. The linear relationship between the amount of immunoreactive protein on the membrane and the fluorescence intensity detected by the infrared detection system (LI-COR Biotechnology)[21,22] allows direct and quantitative comparisons between the ratio of two proteins across multiple blots. Relative amounts of the opsins were calculated by dividing the intensity of the M- or S-opsin band by the intensity of the β-actin band. The average of the WT younger samples was set as 100%.[8]

Immunohistochemistry (IHC)

Materials and methods were previously published for IHC.[16] Briefly, the retinal sections were obtained from the eyes fixed in 4% paraformaldehyde in PBS for 1 hour on ice. Each lens was removed prior to embedding in optimal cutting temperature (OCT) medium (Sakura Finetechnical Co., Ltd., Torrance, CA, USA) and snap frozen in liquid nitrogen. Frozen retinal sections were cut in a cryostat at 10-μm thickness along the vertical meridian through the optic nerve and were placed on glass slides (three sections per slide, SuperFrost Plus; VWR International, Radnor, PA, USA).

Sections were rehydrated in PBS and blocked with blocking buffer (10% ChemiBlocker, 0.5% Triton X-100; Millipore Corp., Billerica, MA, USA) for 30 minutes at room temperature, then incubated at 4°C overnight with affinity purified rabbit polyclonal antibodies for anti- mouse S- or M-opsin peptide (dilution 1:1000).[16] Sections were washed three times in PBS

Investigative Ophthalmology & Visual Science

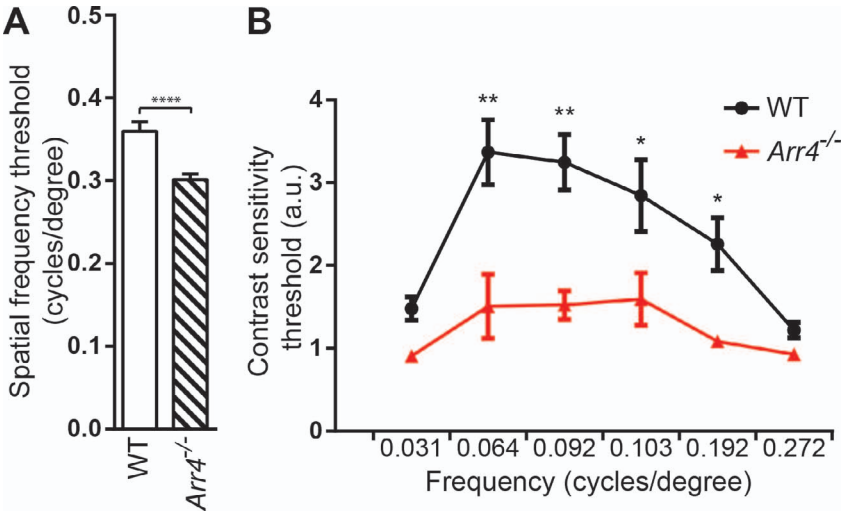

Figure 1. **(A)** Visual acuity thresholds of 4-month-old WT mice compared with *Arr4*$^{-/-}$ mice. Mice that are *Arr4*$^{-/-}$ have a significantly lower visual acuity threshold than WT mice ($P < 0.001$). **(B)** Contrast sensitivity thresholds (arbitrary units = a.u.) of 4-month-old WT and *Arr4*$^{-/-}$ mice at multiple frequencies (cyc/deg). At all midrange frequencies, *Arr4*$^{-/-}$ mice display lower contrast sensitivity thresholds compared with WT. $^{*}P < 0.05$. $^{**}P < 0.01$.

and incubated for 1 hour at room temperature in AlexaFluor 488-conjugated anti-rabbit secondary antibody (1:500; Invitrogen, Carlsbad, CA, USA), then mounted with mounting medium with DAPI (Vectashield, Vector Laboratories, Burlingame, CA, USA) and covered with a glass coverslip.

The same IHC procedures described above were used for whole-mount immunological analysis, except for the following antibody incubation times: primary and secondary antibodies were each sequentially incubated for 36 hours. Slides were viewed and imaged using either a Leica DMR fluorescent microscope (Leica Microsystems, Buffalo Grove, IL, USA) using a ×20 dry lens or a confocal microscope (Carl Zeiss LSM-510; Carl Zeiss Microscopy, Jena, Germany) with a ×40 oil immersion lens equipped with a digital camera (SPOT SP401–115, software version 3.5; Diagnostic Instruments, Inc., Sterling Heights, MI, USA).

Intensity Measurements

Images were recorded using the digital camera with identical exposure times for all retinas studied. The average pixel intensity of the photoreceptor layer was quantified in ImageJ[23] (http://imagej.nih.gov/ij/; provided in the public domain by the National Institutes of Health, Bethesda, MD, USA) at equally spaced regions across each retina section, from the ON to 2.1 mm away in either direction (inferior and superior).

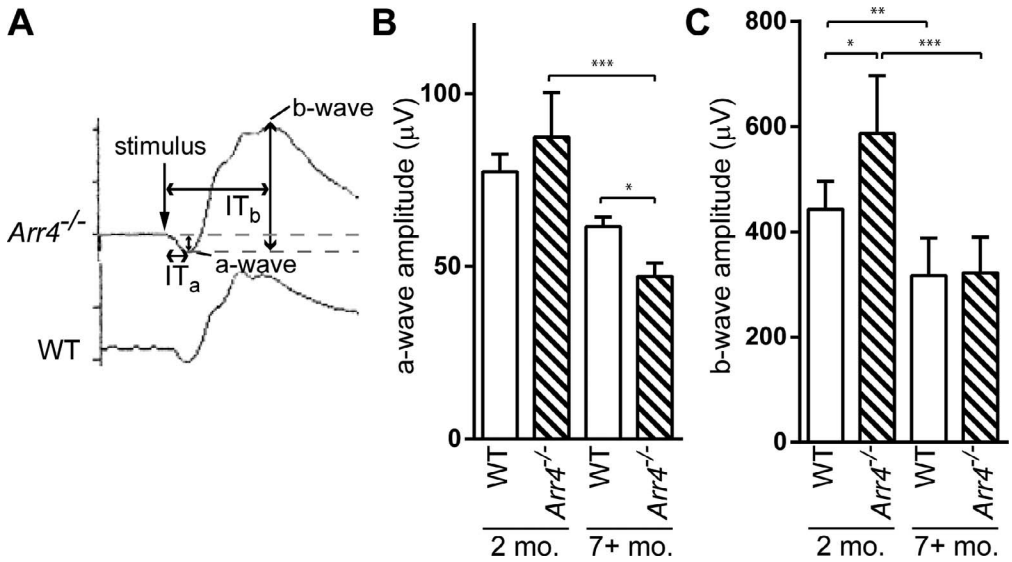

Figure 2. **(A)** Representative photopic ERG tracings for 2-month-old *Arr4*$^{-/-}$ and WT mice; IT_a is the implicit time, or the time from the stimulus to the peak of the wave, for the a-wave; IT_b is the implicit time for the b-wave. **(B)** A-wave amplitudes of younger (2 months) and older (≥7 months) WT and *Arr4*$^{-/-}$ mice. Older *Arr4*$^{-/-}$ mice have significantly lower amplitudes than younger *Arr4*$^{-/-}$ mice ($^{***}P < 0.001$) and older WT mice ($^{*}P < 0.05$). **(C)** B-wave amplitudes of younger and older WT and *Arr4*$^{-/-}$ mice. Younger *Arr4*$^{-/-}$ mice have significantly higher b-wave amplitudes ($^{*}P < 0.05$), while older *Arr4*$^{-/-}$ b-wave amplitudes are significantly decreased compared with younger *Arr4*$^{-/-}$ amplitudes ($^{***}P < 0.001$). Amplitudes of WT also decrease with age. $^{**}P < 0.01$.

Cone Cell Counts

Confocal micrographs of the whole-mounted retinas (n = three animals per group) were taken at the focal level of the outer segments of M- and S-opsin immunologically stained cones, covering a 300×300 um^2 area at both the superior and inferior regions (1 mm away from optic disc) of the retina. Each cone outer segment was then marked by a visual dot, using photo editing software (Photoshop; Adobe Systems, Inc., Mountain View, CA, USA), to facilitate accurate counting.

Outer Nuclear Layer Thickness Measurement

Staining with DAPI was performed as described for IHC above. The fluorescence of DAPI for each entire retina section was captured using a fluorescent microscope (×20 objective, Leica DMR; Leica Microsystems) with a SPOT imaging program. Images were stitched together with photo editing software (Adobe Systems, Inc.) to recreate the whole vertical section of the retina. Starting 0.3 mm from the optic nerve, the number of layers of nuclei were counted[7] every 0.6 mm on both the inferior and superior sides of the retina.

Statistical Analysis

Statistical analysis was performed using two-way ANOVA and Student's *t*-tests with graphing software (GraphPad Prism 6; GraphPad Software, Inc., La Jolla, CA, USA) or three-way ANOVA with statistical software (SPSS Statistics, IBM Corp., Armonk, NY, USA). Huynh-Feldt correction factors were used when the data failed the Machly's test of sphericity. Post-hoc tests were performed using Student's *t*-tests with rough false discovery rate correction factor[24] to decrease the chance of Type II Errors.

Results

OKT Studies Reveal Decreased Visual Acuity and Contrast Sensitivity in *Arr4*$^{-/-}$ Mice

Based on our original hypothesis that visual acuity or contrast sensitivity would be compromised in *Arr4*$^{-/-}$ mice, OKT was used to measure visual acuity and contrast sensitivity in *Arr4*$^{-/-}$ mice compared to WT. Spatial frequency and contrast sensitivity thresholds are commonly used as measurements of functional visual performance in rodents. Because data from a previous study noted abnormally high photopic ERG amplitudes in 1-month-old *Arr4*$^{-/-}$ mice,[7] OKT studies were performed to determine the effect of the absence of ARR4 expression on visual function. Four-month-old *Arr4*$^{-/-}$ mice have significantly reduced visual acuity thresholds compared with WT mice (Fig. 1A; Student's *t*-test $P < 0.001$). The average contrast sensitivity threshold function for each genotype at multiple spatial frequencies (cyc/deg) is shown in Figure 1B. Mice that are *Arr4*$^{-/-}$ have significantly lower contrast sensitivity thresholds than WT mice at all midrange spatial frequencies (two-way repeated ANOVA $F[5,89] = 4.55$, $P < 0.001$).

Physiological Response of Young *Arr4*$^{-/-}$ Mice Is Abnormal Compared to WT

The functional vision deficits displayed in the OKT of 4 month old *Arr4*$^{-/-}$ mice indicate a problem with visual signaling and/or downstream processing, although the photopic ERG recording of 1-month-old *Arr4*$^{-/-}$ mice was abnormally high. We hypothesized that the abnormal signaling would lead to visual deficits in older *Arr4*$^{-/-}$ mice. In order to determine if age-related changes were occurring in the retina, photopic ERGs were performed in age-matched *Arr4*$^{-/-}$ and WT mice aged 2 and ≥7 months.

Representative waveforms to single flash stimuli from light-adapted mice are shown in Figure 2A. In single flash tracings, the a- and b-wave amplitudes are shown (Figs. 2B, 2C). The younger *Arr4*$^{-/-}$ mice display larger photopic ERG amplitude responses compared with WT controls, which is consistent with published results.[7]

Analyses of the a-wave amplitudes showed significant differences in amplitudes between genotypes that were dependent on age (two-way ANOVA interaction effect, $F[1,26] = 5.03$, $P < 0.05$; Fig. 2). We found a significant decrease in a-wave amplitude across age in *Arr4*$^{-/-}$ mice ($P < 0.001$), but not WT mice. The a-wave amplitude in older *Arr4*$^{-/-}$ mice was even significantly lower than older WT mice ($P < 0.05$).

Electroretinogram b-wave amplitudes were significantly decreased in old versus young mice (two-way ANOVA main effect, $F[1,25] = 27.37$, $P < 0.001$), with WT mice decreasing by 28% ($P < 0.01$) and *Arr4*$^{-/-}$ mice by 45% ($P < 0.001$). In addition, younger *Arr4*$^{-/-}$ mice had significantly higher b-wave amplitude than younger WT mice ($P < 0.05$). Our results show that both a- and b-wave amplitudes decrease with age in the *Arr4*$^{-/-}$ mouse.

Representative flicker waveforms are shown in Figure 3A. Younger *Arr4*$^{-/-}$ mice had significantly higher amplitudes compared with older *Arr4*$^{-/-}$ mice at all frequencies (three-way ANOVA, frequency x age interaction $F[2,14] = 4.53$, $P < 0.05$). Thus, flicker ERG responses decrease with age for *Arr4*$^{-/-}$ while WT responses remain unchanged.

Immunoblot Analysis Reveals a Decrease in M- and S-Opsin Expression in Older *Arr4*$^{-/-}$ Mouse Retinas

The decrease in photopic ERG signal in the older *Arr4*$^{-/-}$ mice led us to the hypothesis that M- or S-opsin expression level in the mice may correlate with the observed differences in photopic ERG amplitudes. Immunoblot analysis of total retinal protein was performed in order to test this hypothesis (Fig. 4). Immunoreactive M-opsin protein expression level decreases with age in *Arr4*$^{-/-}$ mice; however, no decrease was observed in WT (two-way ANOVA $F[1,8] = 15.60$, $P < 0.01$; Fig. 4B).

For immunoreactive S-opsin, no significant interaction is observed between age and genotype, but each variable contributes independently to the variation between groups (two-way ANOVA main effects of age $F[1,8] = 37.19$, $P < 0.001$, and genotype $F[1,8] = 43.29$, $P < 0.001$; Fig. 4D). There is a significant difference between younger *Arr4*$^{-/-}$ and older *Arr4*$^{-/-}$ mice ($P < 0.001$), and older WT express more S-opsin than older *Arr4*$^{-/-}$ mice ($P < 0.001$).

M-Opsin Expression Is Increased in the Inferior Retina of Young *Arr4*$^{-/-}$ Mice, but in Older Mice Is Similar to WT

The immunoblot studies determined differences in M- and S-opsin expression in the older *Arr4*$^{-/-}$ mice, but this analysis could not determine whether these changes in protein expression occurred on the inferior region, superior region, or both regions of the retina. In order to test our hypothesis that the change in cellular expression pattern of M- and S-opsin is different in the superior and inferior regions of the retina, IHC studies were done on retinal sections to compare immunological staining intensity in the inferior versus superior retina, as well as at defined distances from the optic nerve. Intensities of M-opsin varied by location, age, and genotype (three-way ANOVA interaction, $F[6,76] = 2.6$, $P < 0.05$). In general, M-opsin intensities were significantly lower in the inferior retina compared to the superior retina across all genotypes and age ($P < 0.001$, Fig. 5). In the inferior retina, younger *Arr4*$^{-/-}$ mice have significantly higher M-opsin intensity than younger WT ($P < 0.05$ or $P < 0.01$) and older *Arr4*$^{-/-}$ mice ($P < 0.01$ or $P <$

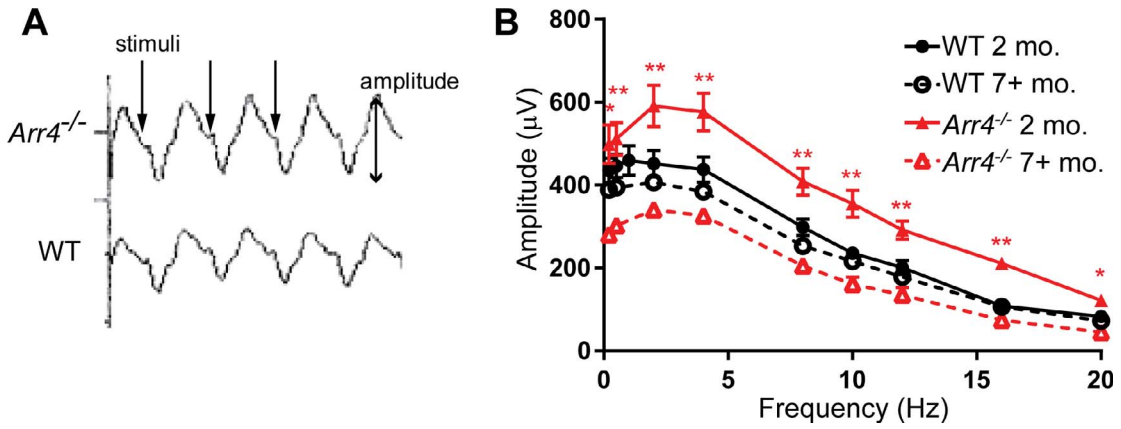

FIGURE 3. (A) Representative photopic response ERG tracings for younger *Arr4*$^{-/-}$ and WT mice with 10-Hz flicker stimulus. (B) Average b-wave amplitudes in response to multiple flicker frequencies. At all frequencies, *Arr4*$^{-/-}$ mice at 2 months of age are significantly higher than *Arr4*$^{-/-}$ mice at 7+ months. $^{**}P < 0.01$. $^{*}P < 0.05$). There are no other significant comparisons.

0.001). In contrast, M-opsin intensity in the WT mice does not change significantly with age.

The overall S-opsin intensities showed an opposite pattern to the M-opsin intensities, with significantly lower intensities in the superior retina (three-way ANOVA, main effect of location $F[4,59] = 36.3$, $P < 0.001$; Fig. 6). No differences in S-opsin intensities for age or genotype were found.

M- and S-Opsin Cone Numbers Decrease With Age in *Arr4*$^{-/-}$ Mouse Retinas

Based on the immunoblot and IHC analysis results indicating that the older *Arr4*$^{-/-}$ mice express less M- and S-opsin, we hypothesized that the older *Arr4*$^{-/-}$ had experienced cone dystrophy, resulting in a decrease in cone number. To clarify if the differences in M- and S-opsin protein expression were due to differential expression in each cone or a difference in total cone number, M- and S-opsin–labeled cone photoreceptor numbers were quantified directly. In mice, M- and S-cones have different expression patterns in the inferior versus superior retina, so these areas were counted separately.[25]

The number of immunoreactive M-opsin cones was significantly different in the superior and inferior regions of the retina with interactions between age and genotype (three-way ANOVA $F[1,8] = 15.6$, $P < 0.01$; Fig. 7A). There are significantly fewer M-opsin cones in the inferior retina of older *Arr4*$^{-/-}$ compared with both younger *Arr4*$^{-/-}$ ($P < 0.001$) and older WT ($P < 0.001$). The pattern is similar in the superior retina, with fewer M-opsin cones in older *Arr4*$^{-/-}$ compared to both younger *Arr4*$^{-/-}$ ($P < 0.01$) and older WT ($P < 0.01$). The number of M-opsin cones in the inferior retina also decreases in WT mice as they age ($P < 0.05$).

The number of S-opsin cones was significantly lower in the superior retina compared with the inferior retina, which depended on genotype or age (three-way ANOVA location *x*

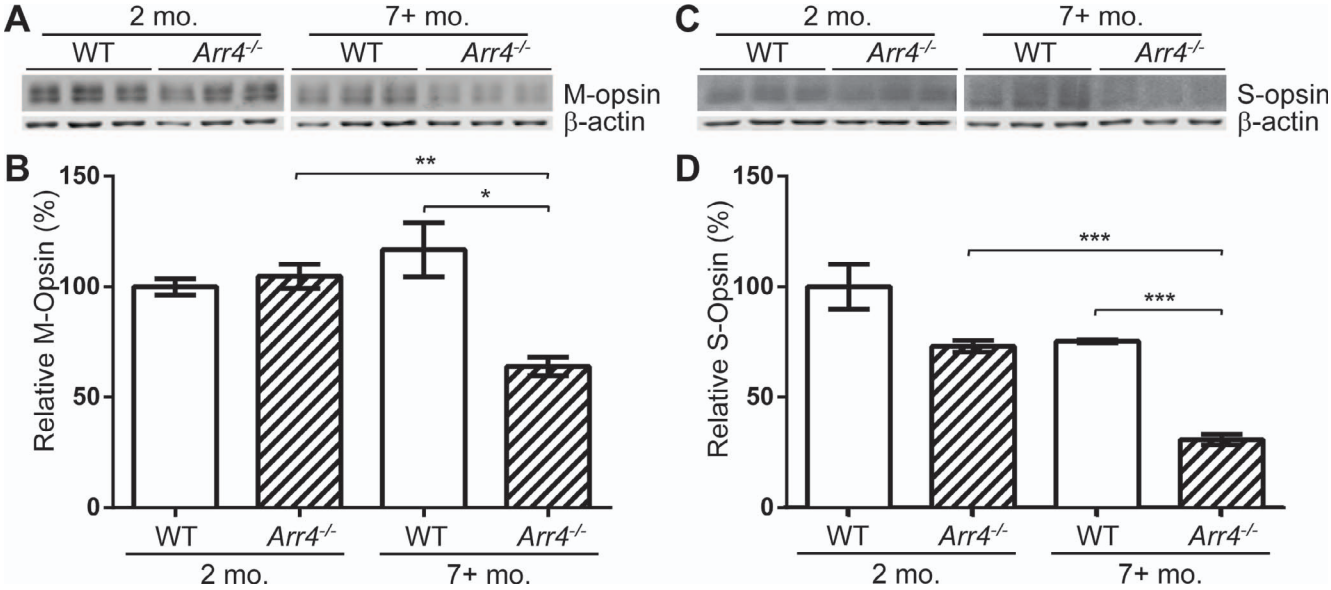

FIGURE 4. (A) Immunoblot analysis of total retinal protein homogenates from SDS-PAGE for three WT and three *Arr4*$^{-/-}$ younger animals (2 months) and older animals (≥7 months). Blot was probed for M-opsin and β-actin expression. (B) Quantification of the intensity of each M-opsin band (see "Methods"). In *Arr4*$^{-/-}$ younger mice, M-opsin is significantly higher than *Arr4*$^{-/-}$ older mice ($^{**}P < 0.01$), and the intensity in WT older mice is significantly higher than *Arr4*$^{-/-}$ older ($^{*}P < 0.05$). (C) Immunoblot analysis of 60 μg of total retinal protein probed for S-opsin and β-actin. (D) Quantification of the intensity of each band. *Arr4*$^{-/-}$ older is significantly lower than *Arr4*$^{-/-}$ younger ($^{***}P < 0.001$) and WT older mice ($^{***}P < 0.001$).

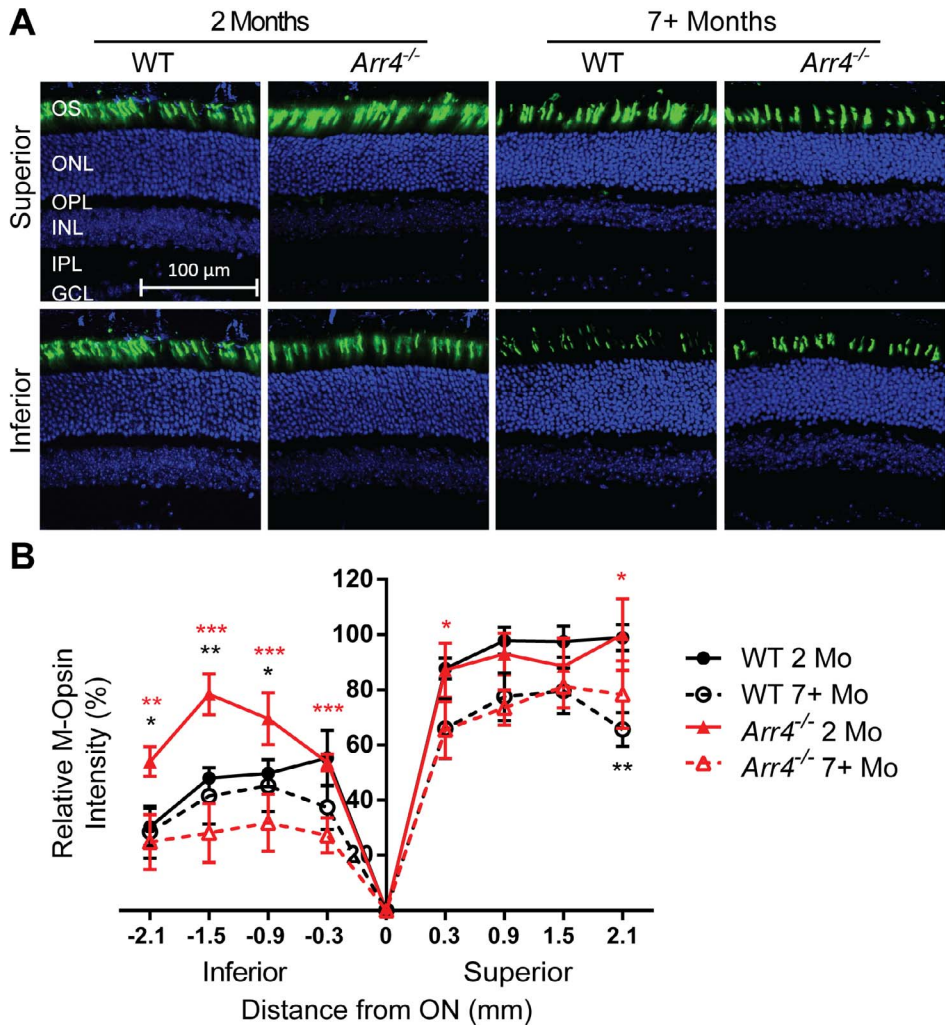

Figure 5. (**A**) Representative images of IHC analysis of retinal sections for M-opsin (*green*). DAPI nuclear stain is in *blue*. (**B**) Quantification of fluorescent intensity of M-opsin IHC staining. Intensities of M-opsin were higher in the superior retina for all ages and genotypes ($P < 0.001$). Additionally, younger *Arr4*$^{-/-}$ mice have significantly higher M-opsin–labeled fluorescent intensity than younger WT mice in the inferior retina ($^{*}P < 0.05$ or $^{**}P < 0.01$). Younger *Arr4*$^{-/-}$ mice have significantly higher M-opsin label fluorescent intensity than older *Arr4*$^{-/-}$ mice throughout the inferior retina as well. $^{**}P < 0.01$. $^{***}P < 0.001$.

genotype $F[1,8] = 9.8$, $P < 0.01$; location x age $F[1,8] = 17.4$, $P < 0.01$; genotype x age $F[1,8] = 9.2$, $P < 0.05$). In the inferior retina, S-opsin cone numbers decrease in both the WT ($P < 0.05$) and *Arr4*$^{-/-}$ ($P < 0.01$) mice across age. Additionally, older *Arr4*$^{-/-}$ retinas have fewer S-opsin cones than older WT retinas in both the inferior ($P < 0.01$) and superior ($P < 0.01$) retina.

We hypothesized that the photoreceptor loss was specific to cones and would not affect the number of rods in the older *Arr4*$^{-/-}$ mice. To determine if the deterioration of cones in older *Arr4*$^{-/-}$ corresponded with an overall degeneration of photoreceptors, including rods, the thickness of the outer nuclear layer of the retina was measured for all groups. We found no significant differences between genotype, age, or location, indicating that the photoreceptor outer nuclear layers remain the same in *Arr4*$^{-/-}$ mice and WT mice across age. The results are consistent with a previous study of young *Arr4*$^{-/-}$ and WT mice.[7]

Discussion

WT Young Versus *Arr4*$^{-/-}$ Young Mice

Visual ARR1 can substitute for ARR4 in both S- and M-opsin mouse phototransduction signal shutoff at the single cell level[8]; however, our results clearly demonstrate that the lack of ARR4 alone contributes to visual phenotype abnormalities. For example, young *Arr4*$^{-/-}$ mice display enhanced photopic ERG b-wave amplitudes (Fig. 2C). We propose that this increase is due, at least in part, to a surprising elevated M-opsin expression in the inferior retina (Fig. 5). Single-cell recordings of cone photoreceptors have confirmed that the expression level of the cone opsins is positively correlated with cone functional signaling.[26,27] In addition, previous work in rodents has indicated that scotopic ERG amplitudes are positively correlated with rhodopsin expression levels,[28,29] so it is feasible to predict that this elevated M-opsin expression would also be correlated with higher photopic ERG amplitudes.

Although patients with enhanced S-cone ERG without widespread retinal degeneration have been reported,[30,31] supernormal cone ERG amplitudes are not commonly observed. When rod phototransduction signaling is compromised,[32–34] enhanced cone ERG amplitudes are observed prior to degeneration and a few molecules even increase photopic ERG amplitudes.[35–39] Enhanced photopic ERG amplitudes have also been observed in rats with streptozotocin-induced diabetes mellitus.[40] Based on these other studies, *Arr4*$^{-/-}$

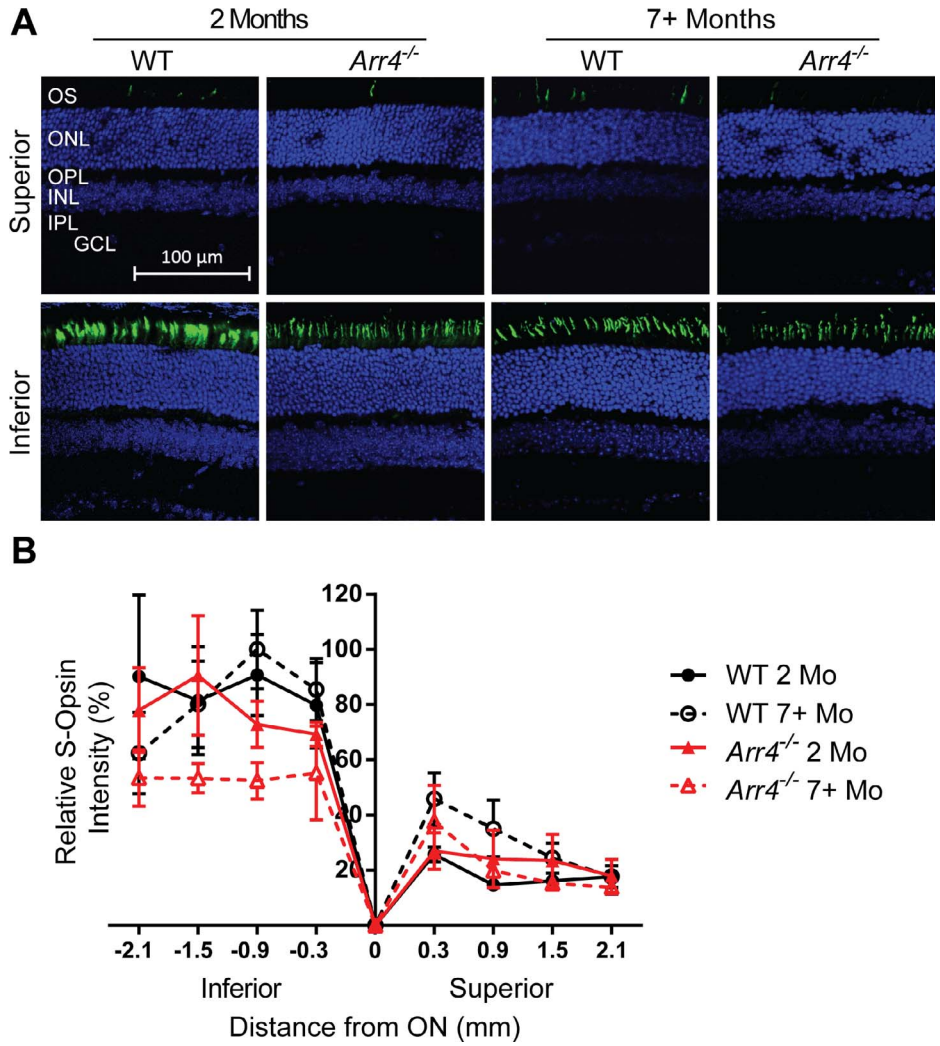

Figure 6. (**A**) Representative images of IHC analysis of retinal sections labeled for S-opsin (*green*); DAPI nuclear stain is *blue*. (**B**) Quantification of IHC fluorescent intensity of S-opsin reveals no significant differences between groups.

visual deficits may provide additional links to understanding the cellular and molecular mechanisms.

In addition, *Arr4*$^{-/-}$ mice performed worse than WT mice in OKT behavioral measurements of visual acuity and contrast sensitivity (Fig. 1). A recent study in zebrafish larvae observed that knockdown of expression of Arr3a, the ARR4 ortholog, causes deficits in optokinetic responses to moving images across many temporal resolutions.[17] These results indicate that cone arrestin is crucial for contrast sensitivity, which in zebrafish is mediated by L- and M-opsin cones,[41,42] and this is consistent with our observation that lack of ARR4 expression in mice leads to a decrease in visual acuity and contrast sensitivity.

There are other rodent models that display defects in optokinetic responses, but usually these functional deficits are accompanied by widespread photoreceptor degeneration, increases in lens opacity, and/or decreases in ERG amplitudes.[43–47] Notable exceptions to this are the amacrine cell-specific tyrosine hydroxylase targeted knockout mouse (rTHKO) and knockout models of two GPCR dopamine receptors, *Drd1* and *Drd4*. *Drd4*$^{-/-}$ mice have a decrease in contrast sensitivity compared to WT, while *Drd1*$^{-/-}$ mice have decreased spatial frequency thresholds compared with WT, and rTHKO display decreases in both contrast sensitivity and visual acuity.[48] It is clear from these data that dopamine and its receptors play an important role in the optokinetic responses, although the molecular mechanism of this process is still under investigation. Recent results indicate that ARR4 plays a role in the desensitization of Drd4, which we hypothesize contributes to the decreased contrast sensitivity observed in both *Arr4*$^{-/-}$ and *Drd4*$^{-/-}$ mice.[49]

While the cellular and molecular mechanisms are still under exploration, the current study demonstrates that expression of normal levels of ARR4 has other modulatory roles in maintaining viable, metabolically healthy cone photoreceptors aside from cone pigment shutoff. Because of the earlier appearance of these visual phenotypes by 2 months, we propose that these roles include developmental triggers and maintenance of daily regulation of cone gene expression. This hypothesis is consistent with our results, which indicate that each M-opsin expressing cone on the inferior side of the young *Arr4*$^{-/-}$ retina produces more M-opsin protein than WT (Fig. 5), while overall M-opsin cone number is not significantly altered in younger *Arr4*$^{-/-}$ mice compared to WT mice (Fig. 7). The immunoblot analysis of M-opsin content did not show an increase in M-opsin in the young *Arr4*$^{-/-}$ retina (Fig. 4A), but we believe that because the increase only occurred in the inferior region of the retina, the difference was not large enough to detect using the total retina homogenate on the immunoblot.

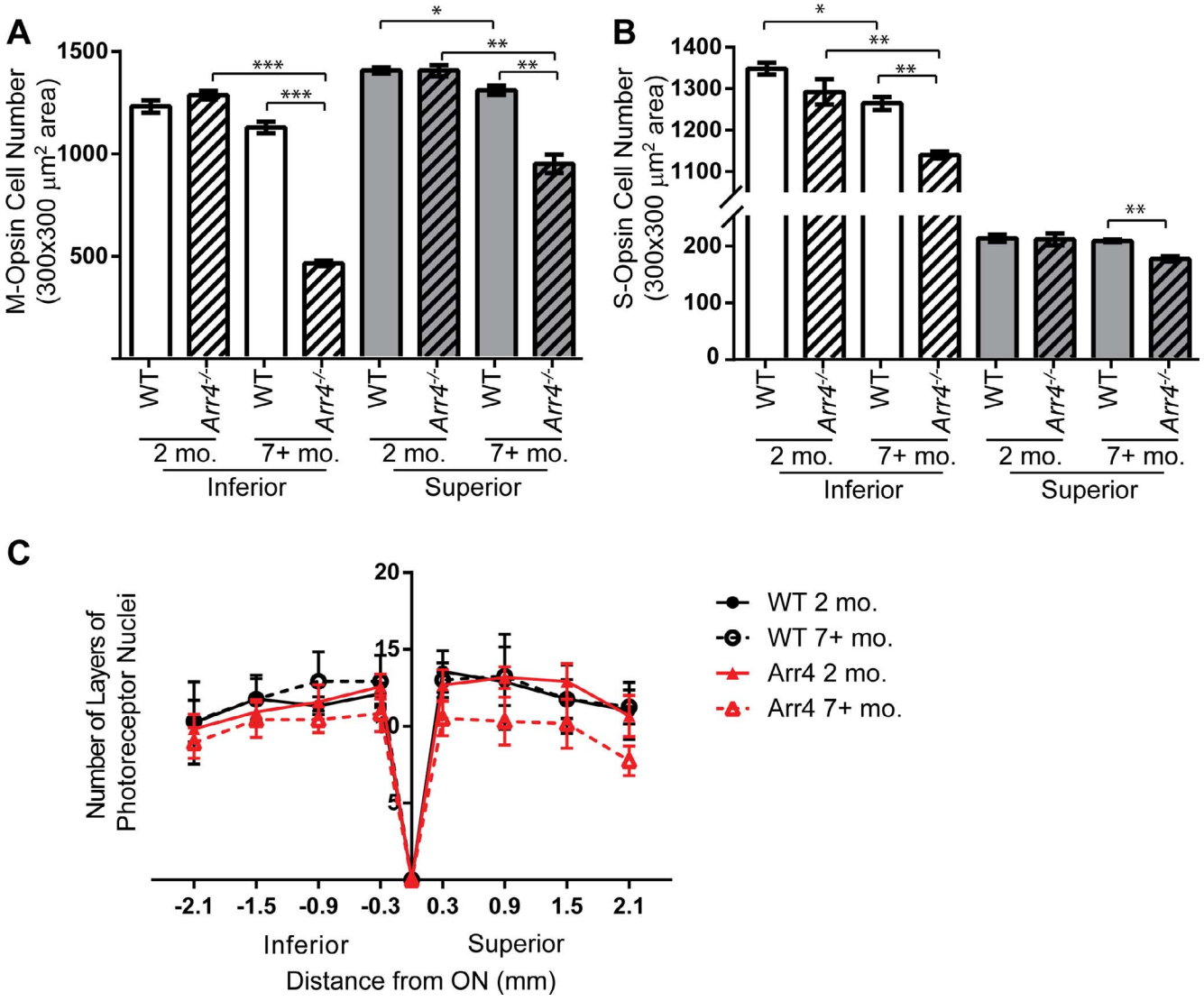

Figure 7. **(A)** Number of M-opsin IHC-stained cones in a 300 × 300 μm² area for young and old WT and *Arr4*$^{-/-}$ mice. Inferior retina regions had fewer M-cones than superior regions. In both the inferior and superior retina, older *Arr4*$^{-/-}$ mice have fewer M-opsin cones than younger *Arr4*$^{-/-}$ mice (***$P < 0.001$, inferior; ***$P < 0.01$, superior) and older WT mice (****$P < 0.001$, inferior; ***$P < 0.01$, superior). In the superior retina, the number of M-cones is decreased in older WT mice compared with WT younger mice (*$P < 0.05$). **(B)** Total number of S-opsin IHC-stained cones in the same area as **(A)**. Superior regions of the retinas had far fewer S-cones than the inferior regions (note *y*-axis split). In the inferior retina, younger mice have significantly more S-opsin cones than older mice for both WT (*$P < 0.05$) and *Arr4*$^{-/-}$ (**$P < 0.01$). The older *Arr4*$^{-/-}$ mice also have significantly fewer S-opsin cones than older WT in both the inferior (**$P < 0.01$) and superior (**$P < 0.01$) regions of the retina. **(C)** Outer nuclear layer thickness, in number of layers of nuclei, throughout the inferior and superior retina. There are no significant differences between groups.

WT Old Versus *Arr4*$^{-/-}$ Old Mice

We also observe clear phenotypes in older *Arr4*$^{-/-}$ mice compared to WT. The total immunoreactive retinal expression of M-opsin and S-opsin is decreased in older *Arr4*$^{-/-}$ mice, while WT remains unchanged (Figs. 5, 6). These data are consistent with the M- and S-opsin cone counts, which reveal an age-dependent degeneration of cone numbers in older *Arr4*$^{-/-}$ mice (Figs. 7A, 7B). In age-matched WT mice, a small but insignificant loss of cones occurs. Follow-up studies were performed to examine hallmarks for cellular apoptosis using TUNEL staining in mouse retina sections at 2, 5, 7, and 9 months, but no significant differences were noted between *Arr4*$^{-/-}$ and WT mice (data not shown). This suggests that the observed cone dystrophy occurs as a gradual degeneration over time. Outer nuclear layer thickness remained consistent with WT for both younger and older *Arr4*$^{-/-}$ (Fig. 7C), indicating that there is no significant rod degeneration. Thus, the degeneration observed in the cones does not affect rod viability and should have no effect on rod structure or function.

Since we observe a significant defect in photopic physiological signaling in the younger *Arr4*$^{-/-}$ mice, the cone dystrophy observed in the older mice may be the result of a slower but cumulative decrease in cone phototransduction shutoff. Alternatively, ARR4 may have other modulatory cellular and developmental partners and interact with GPCR pathways in vivo that are unique and linked to ARR4's functions. Although ARR4 does translocate into the cone outer segments after bright light exposure, a significant amount of ARR4 remains distributed throughout the synapse and the cell body of cones.[50] The reason for this is still unclear, but we hypothesize that ARR4 is essential for performing other critical functions in the cone photorecep-

tor synapse. Arrestin 4 can participate in non-GPCR pathways,[51] and ARR4 has also been shown to interact with a photoreceptor ciliary transmembrane protein, Als2cr4 (TMEM237), which when mutated causes a Joubert syndrome–related disorder.[52,53] This idea is also supported by the ability of ARR4 to bind nonopsin GPCRs, unlike the other visual arrestin, ARR1,[54] so ARR4 is likely to have further functions in cones that have not yet been discovered.

Arr4$^{-/-}$ Younger Versus *Arr4*$^{-/-}$ Older Mice

In our experiments, the greatest phenotypic variations were observed between *Arr4*$^{-/-}$ younger and *Arr4*$^{-/-}$ older groups. Even though the difference is not statistically significant, in photopic ERG recordings and IHC M-opsin intensity measurements, the data values of younger *Arr4*$^{-/-}$ are greater than those observed in the younger WT. For example, the a-wave for younger *Arr4*$^{-/-}$ is consistently higher than that of WT, although the difference does not reach statistical significance (Fig. 2B). However, the older *Arr4*$^{-/-}$ amplitudes are slightly reduced but not significantly different from the older WT. Because of this, there is a significant difference between younger *Arr4*$^{-/-}$ and older *Arr4*$^{-/-}$, but not between younger WT and older WT. This indicates that as these mice age, the *Arr4*$^{-/-}$ mice phenotypically appear more similar to their WT counterparts and may be misinterpreted to have corrected the observed deregulated signaling in younger mice. In fact, if photopic ERGs were only measured in older mice, you would reasonably conclude the ARR4 null mice were physiologically "normal."

In order to investigate this further, we evaluated the overall superior/inferior distribution patterns and their intensity levels of M- and S-opsin expression, in addition to measuring their respective cone cell numbers. In the WT mice, the distribution of M- and S-opsin cones in the inferior and superior retina was consistent with published results.[25] We observed that the older *Arr4*$^{-/-}$ mice have lost M- and S-opsin cones across their entire retinas. In rat models of cone dystrophy, cone number is directly proportional to photopic ERG amplitude.[55] Based on the observed total cone number loss in the older *Arr4*$^{-/-}$ mice, we would predict that the corresponding photopic ERG amplitudes would be lower than older WT mice, but instead we were surprised to observe that the older *Arr4*$^{-/-}$ ERG amplitudes are not significantly different from WT. Despite widespread cone loss, the magnitude of photopic ERG response is similar. These data suggest that each cone photoreceptor is sending an abnormally higher signal postsynaptically for both young and older *Arr4*$^{-/-}$ mice, but the effect is masked by the widespread cone dystrophy in the older animals.

Overall, this investigation leads us to conclude that ARR4 is a key component of normal photopic visual signaling. Mice without ARR4 display widespread cone dystrophy by 7 months of age, indicating that ARR4 is essential for long-term cone survival and high acuity vision over an animal's lifetime. In parallel studies, we are exploring alternative GPCR signaling pathways in cones and potential postsynaptic communication to ON and OFF bipolar and inner retina relays that should reveal how ARR4 is involved in maintaining high acuity vision. Even though no genetic defect has yet been identified for the human *ARR3* X-chromosomal linked cone arrestin, these studies will contribute to a closer examination of patients with deficits in visual acuity and contrast sensitivity or abnormal photopic ERG or flicker responses and may help in understanding the etiology of other cone dystrophies.

Acknowledgments

The authors thank Mary D. Allen (1911–2011) for her lifetime support of Doheny Eye Institute and our vision research program; members of the Mary D. Allen Laboratory for Vision Research, including Lawrence Rife for his technical assistance in ERG recordings, Teresa Ramirez, PhD, and Francis Concepcion, PhD, for assistance in setting up the quantitative morphologic analysis, Erik Haw for genotype analysis, Ernesto Barron for help with confocal imaging, and students Kayleen Lim, Daphne Derose, Nathan Chan, and Harris Liou.

Supported in part by grant awards from National Eye Institute R01-EY015851 (CMC); R01-EY016435 (MTP); EY03040 (Doheny Eye Institute, NEI Core Grant); Department of Veterans Affairs (MTP); Research to Prevent Blindness (USC Ophthalmology); the Mary D. Allen Foundation (CMC, JDD, JSP); Dorie Miller (JDD, JSP); William Hansen Sandberg Memorial Foundation (JDD, JSP); and Tony Gray Foundation (JDD). Cheryl Mae Craft is the Doheny Eye Institute's Inaugural Mary D. Allen Endowed Chair in Vision Research.

Disclosure: **J.D. Deming**, None; **J.S. Pak**, None; **B.M. Brown**, None; **M.K. Kim**, None; **M.H. Aung**, None; **Y.S. Eom**, None; **J. Shin**, None; **E.-J. Lee**, None; **M.T. Pardue**, None; **C.M. Craft**, None

References

1. Pfister C, Chabre M, Plouet J, et al. Retinal S antigen identified as the 48K protein regulating light-dependent phosphodiesterase in rods. *Science*. 1985;228:891–893.
2. Wacker WB, Donoso LA, Kalsow CM, Yankeelov JA Jr, Organisciak DT. Experimental allergic uveitis. Isolation, characterization, and localization of a soluble uveitopathogenic antigen from bovine retina. *J Immunol*. 1977;119:1949–1958.
3. Kuhn H, Hall SW, Wilden U. Light-induced binding of 48-kDa protein to photoreceptor membranes is highly enhanced by phosphorylation of rhodopsin. *FEBS Lett*. 1984;176:473–478.
4. Craft CM, Whitmore DH, Wiechmann AF. Cone arrestin identified by targeting expression of a functional family. *J Biol Chem*. 1994;269:4613–4619.
5. Murakami A, Yajima T, Sakuma H, McLaren MJ, Inana G. X-arrestin: a new retinal arrestin mapping to the X chromosome. *FEBS Lett*. 1993;334:203–209.
6. Chen J, Simon MI, Matthes MT, Yasumura D, LaVail MM. Increased susceptibility to light damage in an arrestin knockout mouse model of Oguchi disease (stationary night blindness). *Invest Ophthalmol Vis Sci*. 1999;40:2978–2982.
7. Brown BM, Ramirez T, Rife L, Craft CM. Visual arrestin 1 contributes to cone photoreceptor survival and light adaptation. *Invest Ophthalmol Vis Sci*. 2010;51:2372–2380.
8. Nikonov SS, Brown BM, Davis JA, et al. Mouse cones require an arrestin for normal inactivation of phototransduction. *Neuron*. 2008;59:462–474.
9. Huang SP, Brown BM, Craft CM. Visual Arrestin 1 acts as a modulator for N-ethylmaleimide-sensitive factor in the photoreceptor synapse. *J Neurosci*. 2010;30:9381–9391.
10. Wilden U, Hall SW, Kuhn H. Phosphodiesterase activation by photoexcited rhodopsin is quenched when rhodopsin is phosphorylated and binds the intrinsic 48-kDa protein of rod outer segments. *Proc Natl Acad Sci U S A*. 1986;83:1174–1178.
11. Baylor DA, Burns ME. Control of rhodopsin activity in vision. *Eye (Lond)*. 1998;12(pt 3b):521–525.
12. Hisatomi O, Matsuda S, Satoh T, Kotaka S, Imanishi Y, Tokunaga F. A novel subtype of G-protein-coupled receptor kinase, GRK7, in teleost cone photoreceptors. *FEBS Lett*. 1998;424:159–164.
13. Weiss ER, Ducceschi MH, Horner TJ, Li A, Craft CM, Osawa S. Species-specific differences in expression of G-protein-coupled receptor kinase (GRK) 7 and GRK1 in mammalian cone photoreceptor cells: implications for cone cell phototransduction. *J Neurosci*. 2001;21:9175–9184.
14. Weiss ER, Raman D, Shirakawa S, et al. The cloning of GRK7, a candidate cone opsin kinase, from cone- and rod-dominant mammalian retinas. *Mol Vis*. 1998;4:27.

15. Chen CK, Zhang K, Church-Kopish J, et al. Characterization of human GRK7 as a potential cone opsin kinase. *Mol Vis*. 2001; 7:305–313.
16. Zhu X, Brown B, Li A, Mears AJ, Swaroop A, Craft CM. GRK1-dependent phosphorylation of S and M opsins and their binding to cone arrestin during cone phototransduction in the mouse retina. *J Neurosci*. 2003;23:6152–6160.
17. Renninger SL, Gesemann M, Neuhauss SC. Cone arrestin confers cone vision of high temporal resolution in zebrafish larvae. *Eur J Neurosci*. 2011;33:658–667.
18. Aung MH, Kim MK, Olson DE, Thule PM, Pardue MT. Early visual deficits in streptozotocin-induced diabetic long Evans rats. *Invest Ophthalmol Vis Sci*. 2013;54:1370–1377.
19. Prusky GT, Alam NM, Beekman S, Douglas RM. Rapid quantification of adult and developing mouse spatial vision using a virtual optomotor system. *Invest Ophthalmol Vis Sci*. 2004;45:4611–4616.
20. Hood DC, Seiple W, Holopigian K, Greenstein V. A comparison of the components of the multifocal and full-field ERGs. *Vis Neurosci*. 1997;14:533–544.
21. Eaton SL, Roche SL, Llavero HM, et al. Total protein analysis as a reliable loading control for quantitative fluorescent Western blotting. *PLoS One*. 2013;8:e72457.
22. Shutz-Geschwender A, Zhang Y, Holt T, McDermitt D, Olive DM. *Quantitative, Two-Color Western Blot Detection With Infrared Fluorescence*. Lincoln, NE: LI-COR Biosciences: 2004.
23. Reish NJ, Maltare A, McKeown AS, et al. The age-regulating protein klotho is vital to sustain retinal function. *Invest Ophthalmol Vis Sci*. 2013;54:6675–6685.
24. Benjamini Y, Hochberg Y. Controlling the false discovery rate: a practical and powerful approach to multiple testing. *J Royal Stat Soc Series B*. 1995;57:289–300.
25. Szel A, Rohlich P, Caffe AR, Juliusson B, Aguirre G, Van VT. Unique topographic separation of two spectral classes of cones in the mouse retina. *J Comp Neurol*. 1992;325:327–342.
26. Daniele LL, Insinna C, Chance R, Wang J, Nikonov SS, Pugh EN Jr. A mouse M-opsin monochromat: retinal cone photoreceptors have increased M-opsin expression when S-opsin is knocked out. *Vision Res*. 2011;51:447–458.
27. Insinna C, Daniele LL, Davis JA, et al. An S-opsin knock-in mouse (F81Y) reveals a role for the native ligand 11-cis-retinal in cone opsin biosynthesis. *J Neurosci*. 2012;32:8094–8104.
28. Goto Y, Peachey NS, Ripps H, Naash MI. Functional abnormalities in transgenic mice expressing a mutant rhodopsin gene. *Invest Ophthalmol Vis Sci*. 1995;36:62–71.
29. Gorbatyuk M, Justilien V, Liu J, Hauswirth WW, Lewin AS. Suppression of mouse rhodopsin expression in vivo by AAV mediated siRNA delivery. *Vision Res*. 2007;47:1202–1208.
30. Sieving PA. 'Unilateral cone dystrophy': ERG changes implicate abnormal signaling by hyperpolarizing bipolar and/or horizontal cells. *Trans Am Ophthalmol Soc*. 1994;92:459–471.
31. Kinori M, Pras E, Kolker A, et al. Enhanced S-cone function with preserved rod function: a new clinical phenotype. *Mol Vis*. 2011;17:2241–2247.
32. Toda K, Bush RA, Humphries P, Sieving PA. The electroretinogram of the rhodopsin knockout mouse. *Vis Neurosci*. 1999;16:391–398.
33. Jaissle GB, May CA, Reinhard J, et al. Evaluation of the rhodopsin knockout mouse as a model of pure cone function. *Invest Ophthalmol Vis Sci*. 2001;42:506–513.
34. Krebs MP, White DA, Kaushal S. Biphasic photoreceptor degeneration induced by light in a T17M rhodopsin mouse model of cone bystander damage. *Invest Ophthalmol Vis Sci*. 2009;50:2956–2965.
35. Popova E, Kupenova P. Effects of dopamine D(1) receptor blockade on the intensity-response function of ERG b- and d-waves under different conditions of light adaptation. *Vision Res*. 2011;51:1627–1636.
36. Popova E. Effects of dopamine receptor blockade on the intensity-response function of electroretinographic b- and d-waves in light-adapted eyes. *J Neural Transm*. 2014;121:233–244.
37. Kapousta-Bruneau NV. Opposite effects of GABA(A) and GABA(C) receptor antagonists on the b-wave of ERG recorded from the isolated rat retina. *Vision Res*. 2000;40:1653–1665.
38. Kim DY, Jung CS. Gap junction contributions to the goldfish electroretinogram at the photopic illumination level. *Korean J Physiol Pharmacol*. 2012;16:219–224.
39. Jurklies B, Kaelin-Lang A, Niemeyer G. Cholinergic effects on cat retina In vitro: changes in rod- and cone-driven b-wave and optic nerve response. *Vision Res*. 1996;36:797–816.
40. Olivier P, Jolicoeur FB, Drumheller A, Lafond G, Zaharia M, Brunette JR. Changes in the B wave of cones and rods in diabetes mellitus induced by streptozotocin in rats [in French]. *Ophtalmologie*. 1990;4:60–63.
41. Krauss A, Neumeyer C. Wavelength dependence of the optomotor response in zebrafish (Danio rerio). *Vision Res*. 2003;43:1273–1282.
42. Orger MB, Baier H. Channeling of red and green cone inputs to the zebrafish optomotor response. *Vis Neurosci*. 2005;22:275–281.
43. Lodha N, Bonfield S, Orton NC, et al. Congenital stationary night blindness in mice - a tale of two Cacna1f mutants. *Adv Exp Med Biol*. 2010;664:549–558.
44. Wright CB, Chrenek MA, Foster SL, et al. Complementation test of Rpe65 knockout and tvrm148. *Invest Ophthalmol Vis Sci*. 2013;54:5111–5122.
45. Wright CB, Chrenek MA, Feng W, et al. The Rpe65 rd12 allele exerts a semidominant negative effect on vision in mice. *Invest Ophthalmol Vis Sci*. 2014;55:2500–2515.
46. Lee CA, Li G, Patel MD, et al. Diabetes-induced impairment in visual function in mice: contributions of p38 MAPK, rage, leukocytes, and aldose reductase. *Invest Ophthalmol Vis Sci*. 2014;55:2904–2910.
47. Aung MH, Park HN, Han MK, et al. Dopamine deficiency contributes to early visual dysfunction in a rodent model of type 1 diabetes. *J Neurosci*. 2014;34:726–736.
48. Jackson CR, Ruan GX, Aseem F, et al. Retinal dopamine mediates multiple dimensions of light-adapted vision. *J Neurosci*. 2012;32:9359–9368.
49. Deming JD, Shin J-A, Lim K, Lee E-J, Van Craenenbroeck K, Craft CM. Dopamine receptor D4 internalization requires a beta-arrestin and a visual arrestin. *Cell Signal*. 2015;27:2002–2013.
50. Zhu X, Li A, Brown B, Weiss ER, Osawa S, Craft CM. Mouse cone arrestin expression pattern: light induced translocation in cone photoreceptors. *Mol Vis*. 2002;8:462–471.
51. Song X, Gurevich EV, Gurevich VV. Cone arrestin binding to JNK3 and Mdm2: conformational preference and localization of interaction sites. *J Neurochem*. 2007;103:1053–1062.
52. Zuniga FI, Craft CM. Deciphering the structure and function of Als2cr4 in the mouse retina. *Invest Ophthalmol Vis Sci*. 2010; 51:4407–4415.
53. Huang L, Szymanska K, Jensen VL, et al. TMEM237 is mutated in individuals with a Joubert syndrome related disorder and expands the role of the TMEM family at the ciliary transition zone. *Am J Hum Genet*. 2011;89:713–730.
54. Sutton RB, Vishnivetskiy SA, Robert J, et al. Crystal structure of cone arrestin at 2.3A: evolution of receptor specificity. *J Mol Biol*. 2005;354:1069–1080.
55. Sugawara T, Sieving PA, Bush RA. Quantitative relationship of the scotopic and photopic ERG to photoreceptor cell loss in light damaged rats. *Exp Eye Res*. 2000;70:693–705.

Investigative Ophthalmology & Visual Science